THE PORPHYRINS

Volume IV

Physical Chemistry, Part B

Edited by

DAVID DOLPHIN

Department of Chemistry
University of British Columbia
Vancouver, British Columbia, Canada

Contents

1   Nuclear Magnetic Resonance Spectroscopy of Diamagnetic Porphyrins

THOMAS R. JANSON AND JOSEPH J. KATZ

2   Nuclear Magnetic Resonance of Paramagnetic Metalloporphyrins

GERD N. LA MAR AND F. ANN WALKER (JENSEN)

7 Electron Spin Resonance and Electronic Structure of Metalloporphyrins

W. C. Lin

8 Mössbauer Spectra of Hemoproteins

Eckard Münck

9 Mössbauer Spectroscopy of Iron Porphyrins

John R. Sams and Tsang Bik Tsin

3

ENDOR Spectroscopy of the Chlorophylls and the Photosynthetic Light Conversion Apparatus

JAMES R. NORRIS, HUGO SCHEER, AND JOSEPH J. KATZ

I. INTRODUCTION

Electron nuclear double resonance (ENDOR) spectroscopy is a high-resolution extension of electron spin resonance (esr) spectroscopy in which two irradiating frequencies are used simultaneously.[1] One of these is at the

resonance frequency of the unpaired electron and the second frequency is for irradiating the magnetic nuclei that may interact with the unpaired electron. As esr has been extensively used in the study of photosynthesis and of related doublet state porphyrin free radicals, the ENDOR technique has become an important and in many cases an indispensible tool for the investigation of porphyrin and metalloporphyrin free radicals both *in vivo* and *in vitro*.

The fundamental impetus for the application of ENDOR to the initial light conversion act of photosynthesis is the special pair model for the primary donor of photosynthesis.[2-12] The special pair model invokes the participation of two molecules of chlorophyll in the primary act of photosynthesis. These are held together in such a manner that both chlorophyll molecules share the doublet state (unpaired) electron, which is produced in the initial act of photosynthesis, and which can be observed by esr. High-resolution ENDOR spectroscopy makes it possible to map the location of the unpaired doublet state electron. Thus, ENDOR can provide explicit data that can serve to support or deny the validity of the special pair model. When applicable, ENDOR is greatly superior to esr for determining whether an unpaired electron is delocalized over one or over two molecules. Although the first direct connection between the doublet species generated in the primary act of photosynthesis and the special pair model was provided by esr investigations,[4] it was ENDOR spectroscopy that provided the more detailed evidence that bears on the special pair proposal.[12] In fact, ENDOR data on photosynthetic bacteria provides the clearest and strongest evidence that a special pair of bacteriochlorophyll molecules function as the primary donor of photosynthesis.[7-12]

In this review we emphasize only proton (^1H) ENDOR spectroscopic studies of the chlorophylls and the photosynthetic apparatus. A detailed theory of ENDOR spectroscopy is omitted as only a brief description of the physical principles of the method is required for a discussion of the various photosynthetic problems thus far elucidated or studied by ENDOR spectroscopy.

II. THEORY OF ENDOR SPECTROSCOPY

To provide a basis for the evaluation of conclusions based on the ENDOR technique, we first review a few aspects of ordinary esr spectroscopy. Only a few key features or principles of magnetic resonance are discussed here, as a number of excellent general treatments of the physics and applications of esr and ENDOR are readily available.[13,14]

A. Hyperfine Interactions

The physical constant of fundamental interest in this review is the electron–nuclear hyperfine (hf) constant, A. Physically, the hyperfine interaction (hfi) may be viewed as a measure of the strength of the magnetic interaction between a magnetic nuclear spin and an unpaired electron spin. The units of A are typically given in terms of gauss (G) or megahertz (MHz). In the magnetic field commonly used for chlorophyll studies, 1 G = ~2.84 MHz. Electron spin resonance spectra of simple compounds or of highly symmetrical compounds can easily be used to extract the hfi constants A_i. A hf constant A_i exists for each ith magnetic nucleus in a given substance. Since A_i is proportional to the "spin density" of the unpaired electron in typical aromatic systems, a knowledge of A_i permits the "mapping" of the delocalized unpaired electron at particular atomic sites in a free radical. The hf coupling constant A_i of the ith nucleus is related to the spin density by the relation[15-18]

$$A_i = Q\rho_i \tag{1}$$

where Q is a constant (~ 30 G for the doublet states of chlorophyll) and ρ_i is the spin density of the unpaired electron interacting with the ith nucleus. The spin density ρ_i represents the fraction of the unpaired or delocalized electron located at a given atom in the framework of the molecule. Thus, a complete mapping of an unpaired electron in terms of hfi provides the information necessary to decide whether one or two molecules house the delocalized unpaired electron produced in the primary act of photosynthesis. Unfortunately, complicated unsymmetrical systems such as are chlorophyll free radicals, and the *in vivo* photosynthetic apparatus do not readily lend themselves to the extraction of hf A_i values by the deconvolution technique. We now describe why this hf information is difficult, if not impossible, to acquire by esr, but is readily available by ENDOR.

B. Esr Technique

For n equivalent nuclei of spin I associated with a delocalized doublet state electron spin there are $2nI + 1$ esr transitions. For many inequivalent groups of equivalent nuclei the number of esr transitions L_{esr} is given

$$L_{esr} = \prod_i (2n_i I_i + 1), \tag{2}$$

where $\prod$ denotes the product symbol and i is a label for each inequivalent group. For bacteriochlorophyll monomer cation doublets, $L_{esr} = 331,776$, assuming hfi with four inequivalent nitrogens, two inequivalent methyl groups, four inequivalent reduced protons of rings II and IV, one C-10

(a)   (b)
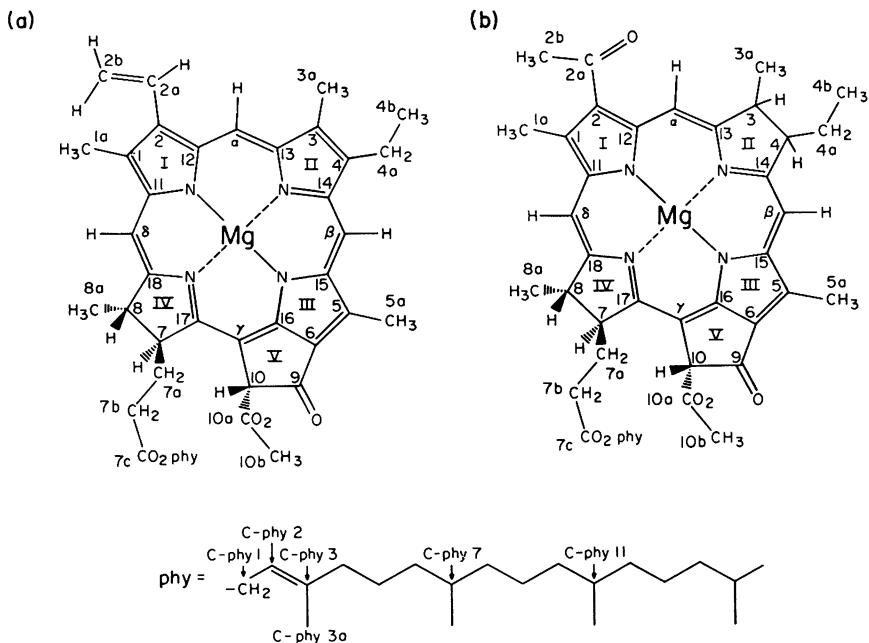
Fig. 1. (a) Chlorophyll *a* (Chl *a*) chemical formula and numbering system. (b) Bacteriochlorophyll *a* (Bchl) chemical formula and numbering system.

proton, and three nonequivalent protons of the bridging methines (see Fig. 1 for the structure and numbering of chlorophyll). Whether these transitions can be resolved by the esr technique can be estimated. In typical doublet state free radicals of aromatic molecules,

$$\sum_i |\rho_i| \simeq 1 \tag{3}$$

where ρ_i is the spin density of the unpaired electron interacting with the ith nucleus. Equation (3) is an oversimplified but essentially correct statement of conservation of unpaired spin. Thus, the more delocalized the unpaired electron becomes as it interacts with a large number of nuclei, the smaller each value of ρ_i becomes.

The total splitting, A_{max}, which differs from the average splitting (ΔH, linewidth) of an esr spectrum is given by

$$A_{max} \simeq 2 \sum_i A_i I_i \tag{4}$$

Combining Eqs. (1) and (3) gives

$$\sum_i A_i \simeq Q \sum_i \rho_i \simeq Q \tag{5}$$

Thus, if $I_i = \frac{1}{2}$, as it does for protons (^{1}H), then according to Eqs. (4) and (5)

$$A_{max} \simeq Q$$

Implicit in the simple derivation of A_{max} is the assumption of isotropic hfi that involve mainly protons. If the hfi also involved nitrogen atoms ($I = 1$), then $A_{max} \simeq 2Q$. If anisotropic h were important, then A_{max} would again be roughly doubled. For our purposes Q is a sufficiently accurate measure of the total spectral width, A_{max}. It has turned out that the significant hf coupling constants do in fact arise mainly from isotropic interactions with protons. Consequently, for the chlorophylls, the maximum spectral width is limited roughly by Q, that is, 25–40 G. Thus, the 331,776 transitions possible in bacteriochlorophyll must occur in a total field range of approximately 25–40 G.

Assuming on the average an equal separation of all esr transitions, it can be seen that the resonances are separated by $\sim 90\ \mu$G (given a maximum total width A_{max} of 30 G). Even under favorable experimental situations, the linewidths of individual hyperfine transitions approach only 10 mG in aromatic systems. Favorable conditions require rapidly rotating, small symmetrical molecules in nonviscous media. Thus, even if we are in error by three orders of magnitude in estimating the number of separate esr transitions, a complete resolution of hyperfine structure in the chlorophylls cannot be expected. Resolution by esr in solid media or in photosynthetic organisms is expected to be even more difficult. In rigid media line broadening of each hf transition occurs and, in many instances where high resolution esr spectra can be recorded in liquid solution, no resolution can be obtained in the solid state. Thus, it is difficult to measure the hf A_i by esr, and thus the location of the delocalized unpaired electron cannot be mapped by esr. Typical esr spectra of the chlorophylls are shown in Fig. 2.

C. ENDOR Technique

Clearly greater resolution must be obtained by a different technique, and ENDOR spectroscopy serves this purpose. In Fig. 3 we illustrate the interaction of a delocalized, unpaired electron with ten nonequivalent groups of equivalent nuclei, that is, the same set of protons used to calculate the value of L_{esr} in Eq. (2) (Section II,B,2). Note that the ten groups of nuclei represented in Fig. 3 do not include interactions with the nitrogen atoms, which as yet have not been observed in chlorophylls by ENDOR spectroscopy. As two of these groups are methyl protons, whereas the remaining eight are single protons, Eq. (2) predicts 4096 esr transitions. By virtue of the fact that the unpaired electron is delocalized, it interacts with 4096 different possible spin configurations of the chlorophyll macrocycle protons. In a
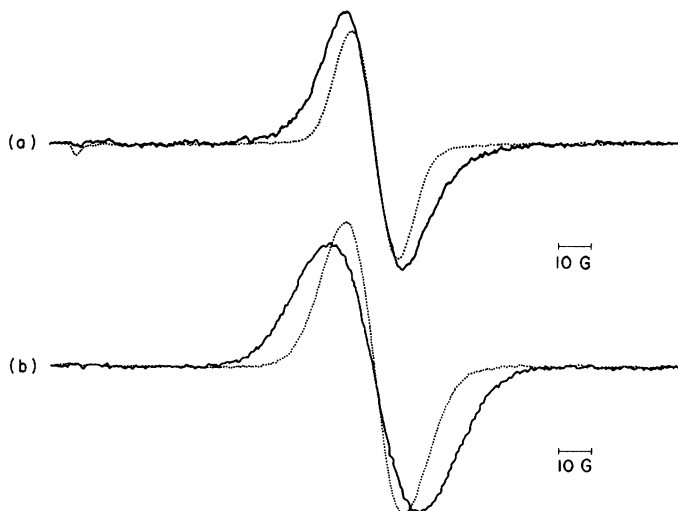
Fig. 2. Typical first-derivative esr signals of the *in vitro* chlorophyll cations (——, labeled *in vitro*) and the *in vivo* light generated doublet Signal I (· · ·, labeled *in situ*): (a) esr signal from Chl a^+; (b) esr signal from oxidized Bchl$^+$
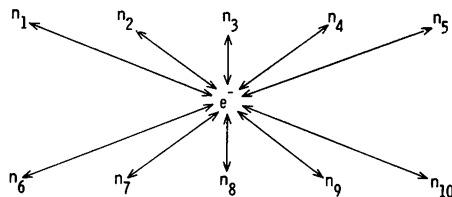
Fig. 3. Graphical representation of a doublet, highly delocalized electron interacting with ten inequivalent groups of nuclei. Note that each group of nuclei interacts only with the electron such that the nuclear environment is simple. In contrast, the delocalized electron interacts with all ten nuclear groups and thus the electron environment is complicated.

given molecule only one combination of nuclear spins occurs at a given instant, but with the large number of molecules in a typical esr or ENDOR experiment, all nuclear spin configurations occur with a population distribution that is statistically predictable. Our ten groups of protons have 4096 different ways to align their nuclear magnetic moments along the magnetic field producing 4096 different local environments for the unpaired electron.

In reality the electron (and thus the esr experiment) also experiences environmental differences produced by other magnetic nuclei (such as nitrogen), as explained in Section II,B, that is, $L_{esr} = 331,776$. Thus, the 4096 proton environments are a gross underestimate of the nuclear environments that interact with the unpaired electron. Nevertheless, the ENDOR

transitions arising from proton interactions are the most significant, and we have therefore calculated only the number of possible proton environments. Even 4096 hfi are sufficient to illustrate the essential features of the situation.

To first order each nonequivalent group of protons i gives rise to two distinct ENDOR transitions at frequencies

$$\nu_i = \nu_{^1H} \pm \tfrac{1}{2}A_i \tag{6}$$

where $\nu_{^1H}$ is the resonance frequency of the proton(s) not coupled to the unpaired electron, that is, the "free" proton frequency. Similar equations govern the ENDOR resonances of other nuclei; the corresponding free nuclear resonance frequency for ^2H and ^{14}N is considerably lower than is $\nu_{^1H}$. Consequently, these nuclei have resonances sufficiently separated from the ^1H atoms that ^2H and ^{14}N need not be taken into account in predicting the ENDOR resolution of the protons, whereas such interactions are important in estimations of esr resolution. Because of the large differences in the "free" atom frequencies, some enhancement in resolution results in ENDOR spectroscopy.

More important, however, is the simplification of ENDOR as compared with esr spectra. According to Eq. (6) each group of n equivalent protons produces only **two** ENDOR lines compared with $n + 1$ esr lines, and the total number of ENDOR resonances is given by a simple sum rather than a product function, as was the case for esr. Thus, the total number of ENDOR resonances generated by m nonequivalent groups of n equivalent nuclei is

$$L_{\text{ENDOR}} = 2m \tag{7}$$

The two transitions per nonequivalent group of n equivalent nuclei correspond to flipping the proton spin in two different resultant magnetic fields in which the unpaired electron field adds to or subtracts from the external (applied) magnetic field. It is clear that the difference in frequency between such a pair of resonances is determined by the strength of the magnetic field produced by the unpaired electron at a given nucleus. A set of two proton ENDOR resonances is centered about the free proton frequency and the separation of resonances (in megahertz or gauss) is a direct measure of the hf constant A. Each proton in the free radical sees only two magnetic environments and consequently for our ten groups of 14 protons in chlorophyll the proton ENDOR spectrum contains only 20 lines compared to the thousands of esr transitions. Because the ENDOR transitions occur within the same range of frequencies of magnetic field of 30 G (or the equivalent in frequency), resonance can be expected to occur every 1.5 G. Since typical isotropic, solid state ENDOR linewidths are ~ 0.4 G, it is reasonable to expect extensive resolution in the ENDOR spectrum of chlorophyll.

It is a fortunate circumstance that the high degree of nuclear localization combined with the small magnetic moment of nuclei as compared with the large magnetic moment of the free electron results in negligible nuclear–nuclear interactions. Each atomic nucleus interacts to a significant extent only with the magnetic moment of the electron. Thus, when the spins of a group of n equivalent, stationary nuclei are "flipped" by the applied radio frequency, only two distinct magnetic environments are observed. When delocalized electrons are flipped, however, a large number of environments are probed. The simplicity of the nuclear environment is the key to the studies described in this chapter.

III. EXPERIMENTAL ASPECTS OF ENDOR SPECTROSCOPY

A. Instrumentation

In principle, ENDOR spectroscopy is performed with a standard esr spectrometer modified to allow a second (lower) frequency (1–40 MHz) to be applied to the sample simultaneously with the normal esr resonance frequency (~ 9 GHz). In practice, obtaining an ENDOR spectrum is not as straightforward as might be expected. An additional coil of wire is placed surrounding the sample in an ordinary microwave esr cavity. The additional coil (in some cases, inside the microwave cavity; in others, outside the microwave cavity) is driven with intense radiofrequency (rf) power, as much as 1000 W. The standard microwave frequency power used in ordinary esr is only in the milliwatt range. Frequently, the intense rf power used to sweep the nuclear resonances leads to spurious signals by "radiofrequency interference."

In a typical ENDOR experiment the external magnetic field is adjusted so that the system is in esr resonance. Then deliberate but partial saturation of the esr signal is achieved by applying a relatively high microwave power (5–20 mW in typical chlorophyll experiments at $\sim 100°$K). The partially saturated esr signal intensity is then monitored as a function of the second high-powered nuclear decoupling frequency, which is swept through the frequency range 1–40 MHz. When a particular proton or group of protons are brought into resonance by the rf decoupling frequency applied to the sample, saturation of the esr signal is relieved and the esr signal intensity becomes larger. (It is also possible to see ENDOR signals that involve shifts in esr signals that do not result from saturation. Such shifts are not deemed relevant to this review.) Thus, ENDOR can be described as a nuclear magnetic resonance (nmr) experiment on free radicals with an esr spectrometer as the detector.[19]

B. Comparison: Advantages and Disadvantages
of Esr and ENDOR

The recovery from saturation when nuclei are brought into resonance by an appropriate rf is a very complicated phenomenom and not completely understood in many instances. For our purposes it is only important to note that a recovery from esr saturation makes ENDOR a nonlinear form of spectroscopy.[19] The rf power level, the rf magnetic field strength, the temperature, the sample viscosity, the frequency of modulation (of both the magnetic field and the rf power), the variety of nuclei, etc. affect the size of an ENDOR signal. The signal size of an ENDOR signal is not necessarily proportional to the number of nuclei that give rise to the signal. Furthermore, these nonlinear effects can make substantial differences in ENDOR spectra recorded in different laboratories on the same sample.

Albeit nonlinear and complicated in practice, ENDOR spectra allow the measurement of hf constants A_i with relative ease. Simple inspection of an ENDOR spectrum reveals A_i. To determine the values of A_i, it is only necessary to measure the frequency difference between two proton peaks symmetrically located about the free proton frequency. For the chlorophylls,

$$A_i \text{ (in MHz)} \simeq 2.84 A_i \text{ (in G)}.$$

In contrast, in a complicated esr spectrum the splittings between lines is a complicated function of all coupling constants, and in general it requires computer deconvolution or simulation before the hf coupling constants can be extracted from such a spectrum.

The principal advantage of ENDOR spectroscopy is the ease with which it allows the measurement of hf coupling constants that can be related to spin densities, even when esr cannot be used to determine these important constants. The nonlinear response of ENDOR spectral intensity is a serious handicap. Although it is a straightforward matter to measure A_i, it is considerably more difficult to assign a particular set of ENDOR resonances to a particular group of n equivalent nuclei. In part, this difficulty is a direct reflection of the inability to use signal intensity as a guide in making assignments since signal size is not directly proportional to the number of nuclei n responsible for the observed ENDOR resonance.

A second important feature of ENDOR associated with nonlinear recovery from saturation is a lower sensitivity for ENDOR compared with esr. As an ENDOR signal measures recovery from saturation, only a small part of the intrinsic esr signal strength is included in an ENDOR signal. ENDOR is typically two or three orders of magnitude less sensitive than esr. If saturation of the esr signal is difficult and the microwave power is increased, then the decoupling rf power must also be increased. In such cases rf power can easily be instrument limited. Furthermore, the signal-to-noise ratio

degrades with either high microwave power or high rf decoupling power. ENDOR is therefore generally carried out at low temperatures (at liquid nitrogen or liquid helium temperatures) to improve ENDOR sensitivity. The sensitivity improvement brought about by low temperatures is related to the increase in the ease of saturation of the esr signal at cryogenic temperatures. Saturation effects are complicated functions of molecular motions. In general the same nonlinear aspects of ENDOR also enter here into the temperature effects and thus are too complicated for discussion in this review. We mention the requirement for low temperatures and the low sensitivity to emphasize that ENDOR spectroscopy also has severe limitations that prevent esr spectroscopy from being displaced.

Clearly the value of ENDOR spectroscopy is enhanced by the application of other standard esr, nmr, electronic transition, and other spectroscopic techniques. To facilitate assignment of the molecular origin of the A_i so easily measured by the ENDOR technique, additional techniques must be invoked, and one of the most powerful of these is selective isotopic labeling, which is discussed in Section V.

IV. EFFECT OF STATE OF CHLOROPHYIL AGGREGATION ON HYPERFINE INTERACTIONS AND ESR LINEWIDTH

Our primary goal in this review is to discuss ENDOR data directly relevant to the photosynthetic process. The utility of ENDOR data proceeds from the extensive esr data acquired over the past two decades on *in vivo* photosynthetic organisms and preparations. Electron spin resonance and ENDOR data complement each other and in practice both are required. Thus, a review of ENDOR is also of necessity a review of a small but crucial portion of the extensive esr literature of photosynthesis.

For many years oxidized chlorophyll has been implicated in the primary act of photosynthesis. As early as 1956 it was known that light produced esr signals in photosynthetic organisms.[20,21] It was suspected that oxidized chlorophyll radicals were produced in the primary step of photosynthesis as the cations of chlorophyll are easily produced *in vitro* by dark chemical reactions and these exhibit esr signals similar to those produced *in vivo* by irradiating photosynthetic organisms with red light.[4,22-28] The *in vivo* generation of free radicals is associated with optical bleaching at ~ 700 nm in green oxygen-evolving plants and bleaching at ~ 870 nm in purple photosynthetic bacteria. Thus, the photoreactive species that give rise to esr signals have been designated as *P*-700 and *P*-865.[29,30] Kinetic measurements on the genesis and decay of the esr signal and of the optical changes

strongly support the view that bleaching at 700 nm (or 865 nm) reflects oxidation of P-700 (or P-865).[31-34] In addition, various kinetic measurements incidate that P-700 and P-865 oxidation occurs in the primary light conversion act of photosynthesis.[35-41]

A. Esr Data on Photosynthesis and Its Interpretation

The four most important esr parameters of *in vivo* photosynthetic systems and *in vitro* chlorophylls that have been studied extensively are the following: (1) the g value (center of the esr resonance); (2) the line shape; (3), the change in linewidth owing to isotopic substitution (^{2}H for ^{1}H and ^{13}C for ^{12}C); and (4) the peak-to-peak first-derivative linewidth, ΔH. These important esr features are listed in Tables 1 and 2 for several systems.

The observed g value of ~ 2.0025 is very near that of the free electron g value of 2.0023. This indicates that the source of the esr signal in photosynthetically important systems is basically an aromatic hydrocarbon whose

TABLE 1
Typical *In Vitro* Chlorophyll Cation esr Data

Species	ΔH isotope ratio[d]	g value	Gaussian line shape[a]	ΔH^b (G)	Isotope[c]	Ref.
Chlorophyll a^e	1	2.0025 ±0.0002	Yes	9.3 ±0.3	^{1}H	4
	2.45	2.0025 ±0.0002	Yes	3.8 ±0.2	^{2}H	4
	0.61	—	No[f]	15.2 ±0.5	^{13}C	6
Bacteriochlorophyll a^g	1	2.0025 ±0.0001	Yes	12.8 ±0.5	^{1}H	4, 23
	2.37	2.0026 ±0.0001	Yes	5.4 ±0.2	^{2}H	4, 23

[a] "yes" indicates that the line shape is very nearly Gaussian.

[b] ΔH is the peak-to-peak linewidth of the first derivative esr absorption spectrum.

[c] ^{1}H indicates normal isotopic composition. ^{2}H indicates $>99\%$ incorporation of ^{2}H instead of ^{1}H. ^{13}C indicates incorporation of $\sim 96\%$ ^{13}C instead of ^{12}C. Only a single isotope is altered from normal.

[d] ΔH isotope ratio $= \Delta H_{^1H}/\Delta H_{\text{isotope}}$.

[e] Chlorophyll cations were prepared by oxidation with I_2 or $FeCl_3$ in CH_3OH or $CH_3OH-CH_2Cl_2$.

[f] Even though the line shape deviates greatly from Gaussian, the different line shape of ^{13}C enriched chlorophyll cations remains essentially identical with that of the *in vivo* light generated esr signal.

[g] Bacteriochlorophyll cations were prepared by oxidation with I_2 in $CH_3OH-glycerol$.

TABLE 2

Data from Typical *in Vivo* Photosignals[a]

Species	ΔH isotope ratio[f]	g values[b]	Gaussian line shape[c]	ΔH[d] (G)	Isotope[e]	Ref.
Syneccochocus lividus	1	2.0025 ±0.0002	Yes	7.1 ±0.2	[1]H	4
	2.41	2.0025 ±0.0002	Yes	2.95 ±0.1	[2]H	4
	0.55	—	No[g]	13.0 ±0.5	[13]C	6
Chlorella vulgaris	1	2.0025 ±0.0002	Yes	7.0 ±0.2	[1]H	4
	2.6	2.0025 ±0.0002	Yes	2.7 ±0.1	[2]H	4
Scenedesmus obliquus	1	2.0025 ±0.0002	Yes	7.1 ±0.2	[1]H	4
	2.6	2.0025 ±0.0002	Yes	2.7 ±0.2	[2]H	4
Rhodospirillum rubrum	1	2.0026 ±0.0001	Yes	9.5 ±0.5	[1]H	4, 23
	2.3	2.0026 0.0001	Yes	.2 0.3	[2]H	4, 23

[a] Esr photosignal is called Signal I in plants.

[b] g Values have been determined since the work of Norris *et al.*[4]

[c] "Yes" indicates that the line shape is very nearly Gaussian.

[d] ΔH is the peak-to-peak linewidth of the first derivative esr absorption spectrum.

[e] [1]H indicates normal isotopic composition. [2]H indicates 99% replacement of ^{1}H by [2]H. [13]C indicates 96% replacement of ^{12}C by [13]C. Only a single isotope is altered from normal.

[f] ΔH isotope ratio = $\Delta H_{1_H}/\Delta H_{\text{isotope}}$.

[g] Even though the line shape deviates greatly from Gaussian, the different *in vivo* line shape of ^{13}C enriched organism remains essentially identical with that of the *in vitro* [13]C enriched monomeric chlorophyll cations.

unpaired electron is "free" in the sense that it does not occupy oxygen and nitrogen sites to any significant extent.

The esr line shape is Gaussian and is consistent with a high and fairly even delocalization of the unpaired electron over the entire π system of the macrocycle. The line shape and the linewidth observed *in vitro* or *in vivo* chlorophyll systems are typical of organic aromatic doublet state free radicals whose esr properties originate from electron–nuclear hf splittings too numerous to be resolved in an esr experiment (see Section II,B). If a single hf coupling constant were significantly larger than the others, an observable splitting would

occur, and a Gaussian line shape would not be observed. Thus, approximate equality in hfi is required, indicating extensive and mostly equal unpaired spin density delocalization.

The linewidth is consistent with an origin of the line shape in a delocalized system both *in vivo* and *in vitro*. Organisms of unusual isotopic composition have been used to determine the origin of the esr signal. These organisms contain ^{2}H or ^{13}C and are obtained by biosynthesis in either a ^{2}H$_2$O medium or with ^{13}CO$_2$ as a substrate. ^{2}H has a smaller magnetic moment than does ^{1}H, and, thus, consistent with extensive electron delocalization over the macrocycle, the linewidths both *in vivo* and *in vitro* are narrowed by a factor ~ 2.4 in ^{2}H systems.[4,6] Because ^{12}C has no magnetic moment, we expect and do observe increases in ΔH on ^{13}C incorporation into the chlorophyll of a photosynthetic organism.

The last esr property we discuss is the linewidth ΔH. Linewidth measurements have provided critical information about the origin of the esr signal in photosynthetic organisms. The linewidth observed *in vivo* is similar to but significantly more narrow than the ΔH of *in vitro* monomer chlorophyll cations, Chl$^{\dotplus}$. Recall that the g value, line shape and (percentage of) change in linewidth upon isotopic substitution are essentially identical in the *in vivo* photo–esr signals and in the *in vitro* cation chlorophyll signals. This supports the view that the *in vivo* esr signal probably arises from a cation free radical of chlorophyll. Only the ΔH values indicate that a difference exists between *in vivo* systems and *in vitro* systems (see Table 3). Originally this difference in linewidth was attributed to a "special environment" that occurs *in vivo* and somehow narrows the linewidth of a Chl$^{\dotplus}$ cation monomer by about 40%. We now believe that this "special environment" is produced by a special aggregation state of chlorophyll *a in vivo*, that is, special pair formation, Chl$_{sp}$.

B. Aggregation Effects on Hyperfine Constants and Esr Linewidths

It is well known that the chlorophylls undergo a variety of aggregation interactions. Since the basic aspects of these aggregation effects are extensively covered in a review by Katz,[42] we now only discuss consequences of aggregation relevant to magnetic resonance investigations by esr or ENDOR.

Aggregation of the chlorophylls can be expected to cause at least two significant changes. First, the optical spectrum of the chlorophyll will be shifted by chlorophyll–chlorophyll interactions. Monomeric acceptor Chl *a* (Chl *a*·L$_1$ or L$_2$, where L is a nucleophile) absorbs at ~ 663 nm, and the *in vivo* species absorbs at 700 nm. This spectral shift is consistent with some sort of chlorophyll aggregation. A similar situation exists in photosynthetic

TABLE 3

Comparison of *in Vivo* and *in Vitro* esr Linewidths[a]

		ΔH			Aggregation
Species	Isotope[b]	Observed	Predicted[c]	Ratio[d]	number[e] (N)
Syneccochocus lividus	^{1}H	7.1 ± 0.2	6.6 ± 0.3	1.08 ± 0.06	1.7
	^{2}H	2.95 ± 0.1	2.7 ± 0.1	1.10 ± 0.05	1.7
	^{13}C	13.0 ± 0.5	12.2 ± 0.5[f]	f	f
Chlorella vulgaris	^{1}H	7.0 ± 0.2	6.6 ± 0.3	1.06 ± 0.05	1.8
	^{2}H	2.7 ± 0.1	2.7 ± 0.1	1.00 ± 0.05	2.0
Scenedesmus obliquus	^{1}H	7.1 ± 0.2	6.6 ± 0.3	1.08 ± 0.06	1.7
	^{2}H	2.7 ± 0.1	2.7 ± 0.1	1.00 ± 0.05	2.0
Rhodospirillum rubrum	^{1}H	9.5 ± 0.5	9.1 ± 0.4	1.05 ± 0.07	1.8
	^{2}H	4.2 ± 0.3	3.8 ± 0.1	1.10 ± 0.09	2.0

[a] Based on data from Tables 1 and 2 and Norris *et al.*[4]

[b] See footnote c of Table 1.

[c] Peak-to-peak linewidth ΔH is predicted from Eq. (13) using $N = 2$ and ΔH_1 as listed in Tables 1 and 2.

[d] Ratio of $\Delta H_{in\ vivo}/(\Delta H_{in\ vitro}/\sqrt{2})$. The *in vitro* values are in Tables 1 and 2. A ratio of 1 indicates that the pair model accounts for the esr data.

[e] $N = (\Delta H_{in\ vitro}/\Delta H_{in\ vivo})^2$.

[f] Owing to the non-Gaussian line shape, Eq. (13) does not apply as discussed in Norris *et al.*[6] Instead the predicted value is based on $\Delta H_{in\ vivo} \cong \Delta H_{in\ vitro}/1.26$ where a special pair is assumed *in vivo* and a monomer is assumed *in vitro*.

bacteria, where large spectral changes are observed *in vivo*. Second, the esr linewidth will be narrowed if the aggregation process allows the unpaired electron to "delocalize" on more than one chlorophyll molecule. Since the esr linewidth is $\sim 40\%$ smaller *in vivo* than *in vitro*, aggregation is also suggested by the available esr data (a possible exception is *Rhodopseudomonas viridis*). To use the reduction in linewidth in the *in vivo* systems, we now develop a formalism that relates the linewidth of the monomer Chl$^+$ to that of chlorophyll aggregate size.[4]

As the extent of delocalization increases, the esr linewidth of the envelope of hyperfine resonances becomes narrower. The peak-to-peak linewidth of monomeric Chl, ΔH_1, of a Gaussian first-derivative esr curve is related to the electron nuclear hyperfine coupling constants A_i by

$$\Delta H_1{}^2 = \sum_{i=1}^{n} C_i A_i{}^2 + \Delta \tag{8}$$

where C_i is a constant, depending only on nuclear spin, n is the total number of magnetic nuclei in a monomer cation, and Δ accounts for contributions

to the linewidth other than hyperfine interactions, that is, g anisotropy and the intrinsic linewidth associated with each hyperfine transition. A more complete and rigorous treatment has been given in the original derivation.[4] Here we assume isotropic coupling constants (A_i), for simplicity. As we pointed out in Section II,B, the majority of the hyperfine interaction in chlorophyll of ordinary isotopic composition is isotropic.

Isotopic substitution experiments[4] with ^2H and variation in microwave frequency (g anisotropy effects increase with frequency, whereas hyperfine broadening does not) indicate that Δ is so small that we can rewrite Eq. (8) more conveniently in the form

$$\Delta H_1{}^2 = \sum_{i=1}^{n} C_i A_{i_1}^2 \tag{9}$$

We now assume that the unpaired electron is shared equally by each member of an aggregate of size N. Thus, each coupling constant A_{i_1} of the monomer is related to the corresponding coupling constant A_{i_N} of the aggregate by the simple relation

$$A_{i_N} = A_{i_1}/N \tag{10}$$

The linewidth of a free radical in a chlorophyll aggregate is given by an analog of Eq. (9):

$$\Delta H_N{}^2 = \sum_{i=1}^{n} NC_i(A_{i_N})^2 \tag{11}$$

where N takes into account the N couplings of value A_{i_N}, and n is the total number of magnetic nuclei in a single molecule. Combining Eqs. (10), (11), and (9), we see that

$$\Delta H_N{}^2 = \sum_{i=1}^{n} NC_i(A_{i_1}/N)^2 = (1/N) \sum_{i=1}^{n} C_i A_i{}^2 = (1/N) \Delta H_1{}^2 \tag{12}$$

Thus,

$$\Delta H_N = (1/\sqrt{N}) \Delta H_1 \tag{13}$$

is our final expression that relates the linewidth of a free radical in an aggregate containing N chlorophyll molecules to the linewidth of monomeric $Chl^{\ddot{+}}$ free radical (ΔH_1).

Electron spin resonance linewidth studies of aggregation depend on Eq. (13) (a $1/\sqrt{N}$ relationship), whereas ENDOR hyperfine coupling constant studies are based on Eq. (10) (a $1/N$ relationship). Obviously the esr equation [Eq. (13)] represents the sum of the consequences of many hyperfine constants changing and is not as specific as the ENDOR equation [Eq. (10)].

Furthermore, note that for each esr equation (one for each distinctly different isotopic composition) many ENDOR equations exist. ENDOR spectroscopy therefore provides the method of choice for determining and establishing an aggregation number for an unpaired spin delocalized over a chlorophyll aggregate. The *in vivo* esr linewidth data analyzed by Eq. (13) strongly supports a value of $N = 2$ for the number of chlorophyll molecules over which the unpaired spin is delocalized (Table 3), and provides the experimental basis for the chlorophyll special pair proposal, Chl_{sp}, for *in vivo* photoreaction center chlorophyll. The value $N = 2$, as can be seen from Table 3, accounts for the *in vivo* linewidths quite accurately.

V. *IN VITRO* ENDOR OF CHLOROPHYLL CATIONS

Before proceeding with determination of an aggregation number *in vivo*, or even addressing the question as to whether aggregation is the correct explanation of the *in vivo* signal, the *in vitro* ENDOR data must be discussed. It is essential to determine values of A *in vitro* for monomeric chlorophyll to validate comparisons with *in vivo* ENDOR data. We therefore now describe the assignment of the major coupling constants in monomeric chlorophyll cation free radicals by ENDOR spectroscopy. Part of this discussion is based on chemical modification and alterations in the isotopic composition of the chlorophylls.[43] Chemical manipulation has been most easily carried out on methyl pyrochlorophyllide *a*, and this compound serves as a suitable stand in for Chl *a*. Physical techniques help identify which ENDOR transitions are associated with particular methyl groups.[11] Isotopic labeling in purple photosynthetic, nonsulfur bacteria by biosynthetic means allows assignment of *in vivo* couplings as well as *in vitro* couplings. This biosynthetic technique, first developed by Katz *et al.*,[44,45] is essential to establish the validity of any model for *in vivo* reaction center chlorophyll based on delocalization of the unpaired spin in the photooxidized reaction center chlorophyll.

A. Classification of ENDOR Protons

To understand the rationale used to select protons for isotopic substitution, it is necessary to understand which nuclei may possibly interact with the unpaired electron. From a large number of esr and ENDOR studies of aromatic molecules, a classification of proton types useful in making such a judgment has emerged.[13] In this discussion we will refer to the two most important groups of protons as alpha protons and beta protons, in agreement

with standard esr spectroscopic terminology. (It is important to note that this usage is quite different from that conventionally used by organic chemists; for designating specific protons the designations in Fig. 1 will be used.) An alpha proton is any proton one sigma bond removed from the conjugated system. Thus, an alpha proton is the closest hydrogen nucleus to the π system, and consequently anisotropic hfi are expected for alpha protons via the anisotropic electron–nuclear dipole interaction. The beta protons are two sigma bonds removed from the conjugated system. Since dipole–dipole interactions fall off very rapidly with distance, beta protons exhibit very little anisotropy. Both alpha and beta protons have an isotropic hfi governed by Eq. (1), where $Q = \sim 30 \ g$. In both cases, ρ_i refers to the spin density of a carbon atom in the conjugated system one or two sigma bonds removed from the particular nucleus under discussion. For a gamma proton, that is, one three sigma bonds removed from the conjugated system, Q is lowered by a factor of at least ten. Thus, beta and gamma protons exhibit hfi splittings in esr or ENDOR spectra by virtue of long-distance isotropic coupling with spin density of the conjugated system. This means that only alpha and beta protons are expected to have significant hfi constants; this is particularly the case for large conjugated systems such as the chlorophyll macrocycle.

Thus, our chemical modifications or isotopic substitutions are primarily aimed at alpha and beta protons. Chemical changes two or three bonds removed from the conjugated system are expected to alter the unpaired spin density distribution of the macrocycle to a negligible extent.

B. Selective Isotopic Labeling

Assignment of an ENDOR resonance to a specific group of protons is most rigorously achieved by selectively altering the isotopic composition of that group. For example, comparison of the ENDOR spectrum of $\text{Chl}^{\ddot{+}}$ of normal isotopic content with the ENDOR spectrum of $5\text{-C}\,^2\text{H}_3\text{Chl}^{\ddot{+}}$ would reveal the coupling constant of the protons in the 5-methyl group. As explained in Section II,C, ^2H has a much smaller ENDOR frequency due to a smaller free nuclear resonance frequency. Thus, for $\text{Chl}^{\ddot{+}}$ the ^2H ENDOR transitions do not appear at all in the ENDOR spectral range of ^1H protons. Hence, if the 5-CH_3 group gives rise to a set of ENDOR transitions, chlorophyll containing $5\text{-C}\,^2\text{H}_3$ will lack the 5-methyl resonance and thus the assignment is made. Chemical modification and isotopic alterations on chlorophyll in general have been confined to Mg-free derivatives, and the problems associated with Mg reinsertion have dictated the choice of a model system rather than chlorophyll itself (Scheme 1).
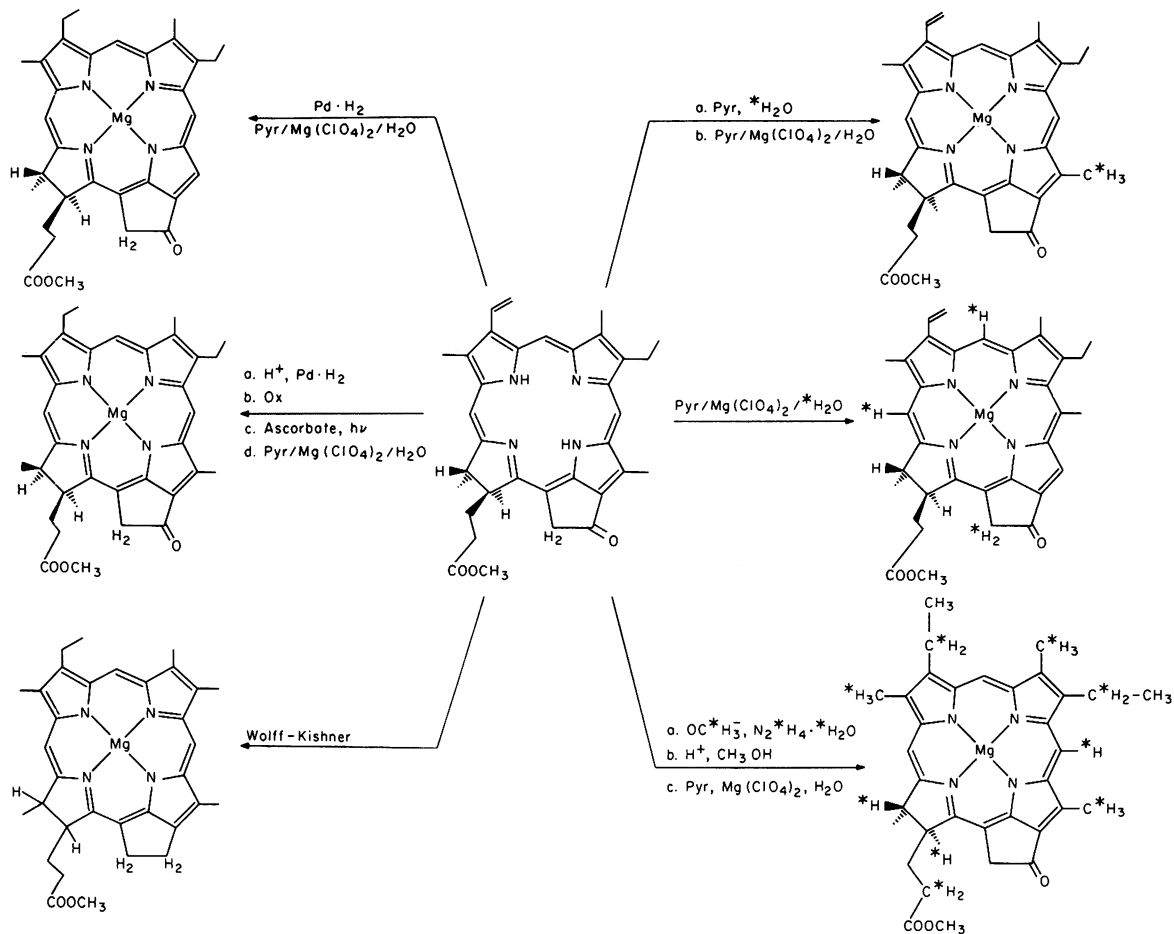
Scheme 1. Reaction scheme for selective deuteration and derivative preparations from methyl pyropheophorbide *a* (compound 2) (Pyr is pyridine).

The choice of a model compound for selective incorporation of ^{2}H was methyl pyrochlorophyllide a (Compound **9**). (See Scheme 2 for the chemical structure for compounds designated by boldface formula numbers enclosed in parentheses.) The ENDOR spectrum of chlorophyll a (Compound **1**), and methyl pyrochlorophyllide a, (Compound **9**), are virtually indistinguishable (Fig. 4), and this establishes methyl pyrochlorophyllide, (Compound **9**), as an appropriate model compound for Chl a, (Compound **1**).

Chl a cation radical exhibits an ENDOR spectrum (Fig. 4a, Table 4) that contains three well-resolved bands (A_1, A_2, A_4) a shoulder (A_3) on the A_2 band, and a broad band (A_5) partially obscured by the A_4 peak. The spectrum is essentially symmetric with respect to the free proton frequency, consistent with observation of interactions with ^{1}H nuclei only. The ENDOR spectrum of methyl pyrochlorophyllide a cation radical (Fig. 4b) is virtually the same as that of Chl a^+. Hence, little spin density interaction is expected with the remote protons of the esterifying alcohol at position C-7b, and the similarity in spectra also suggests small coupling constants and low intensity for the proton(s) at the C-10 position as well.

The major ENDOR line A_4 in model compound 9 essentially disappears with ^{1}H $-$ ^{2}H exchange of the 5-methyl group (see Fig. 5). Thus, the assignment of A_4 to the 5-methyl protons is straightforward in methyl pyrochlorophyllide a, and likewise highly probable in Chl a as well. A methyl group hfi was suspected for A_2 and A_4 on the basis of the ENDOR line shape. For frozen solutions, intense bell-shaped lines have been characteristically associated with rotating methyl groups both from theoretical as well as experimental considerations.[46] Thus, the more definite assignment of A_4 to the 5-CH$_3$ group also reinforces the interpretation of the similarly shaped A_2 resonance as originating from other methyl groups. In Chl a this suggests that 1- and 3-CH$_3$ group proton hfi should be assigned to ENDOR line A_2.

To help validate these assignments Compound **12** was synthesized to contain ENDOR active beta type protons only in the 2- and 4-CH$_2$ and the 1-CH$_3$ groups (i.e., Compound **12b** in Table 4). The ENDOR spectrum of Compound **12b** shows a single resonance corresponding to A_2 in the ENDOR spectra of Chl a, Compounds (9) and 12. Thus, the A_2 and A_3 shoulder probably originate from some or all of the 1- and 3-CH$_3$ protons and the 4-CH$_2$ protons. Mirror-image isotope experiments support these conclusions Exchange of ^{2}H by ^{1}H (in Compound **12**-^{2}H) leads to a significant decrease in A_2 and A_3 versus A_4, corresponding to only partial exchange with ^{1}H of the 1-CH$_3$, 2-CH$_2$, and 4-CH$_2$ deuterons under the exchange conditions.

It is easily demonstrated that none of the observable ENDOR resonances representing significant spin density arise from the α- and β-methine protons and the 10-CH$_2$ protons since ^{2}H substitution in these positions causes no

A

1

B

2,9

C

3,4,8
10,11,12,17

D

5,6,7
13,14,15

E
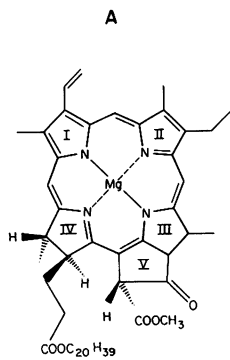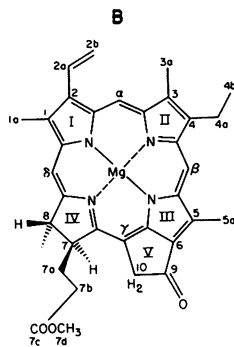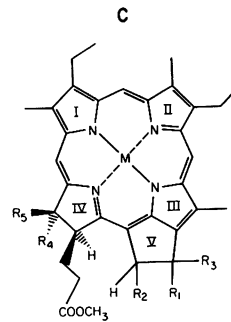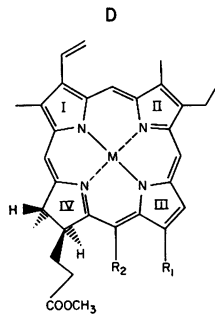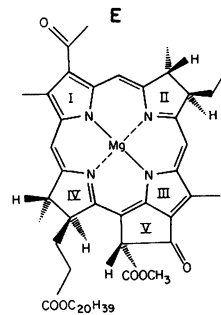
16

Scheme 2

Compound number[a]		Modifications					
Free base (M = H_2)	Chlorophyllide (M = Mg)	R_1. R_3[b]	R_2	R_4	R_5	Remarks	Location
——	1, 1a	——	——	——	——	Chlorophyll a	A
2, 2a, 2b, 2c	9, 9a, 9b	—	——	——	——	Basic Chl a derivative	B
3, 3a	12, 12a, 12b, 12c	=O	H	CH_3	H	—	C
4	10	H_2	H	CH_3	H	Racemic	C
5	14	$COOCH_3$	CH_2COOCH_3	——	—	No ring V No R_3	D
6	15	H	CH_2COOCH_3	—	——	No ring V No R_3	D
7	13	$COOCH_3$	H	——	—	No ring V No R_3	D
8	11	=O	H	H	CH_3	Racemic	C
——	16	—	——	——	——	Bacteriochlorophyll	E
—	17	=O	OH	CH_3	H	C-10 epimers	C

[a] 1a, 2a, 2b, etc. refer to the corresponding compound with isotopic alterations.

[b] Compounds 5, 6, 7, 13, 14, and 15 contain no R_3 group.

[c] In the free base Mg has been replaced by H_2.
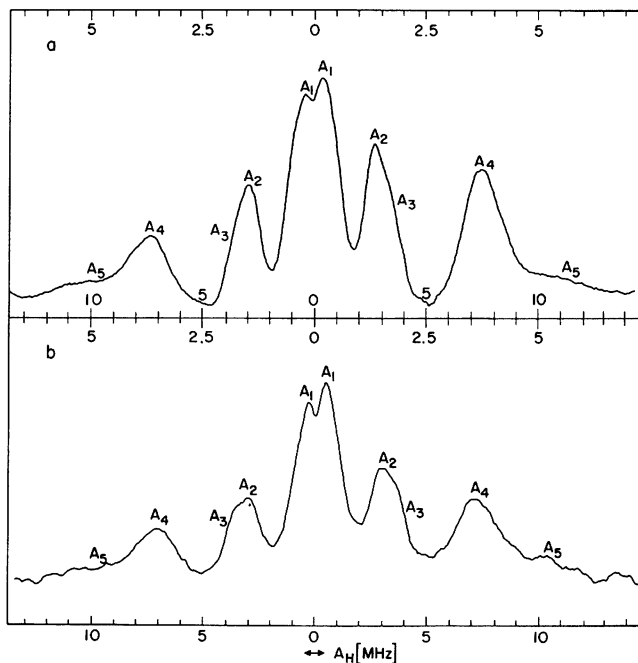
Fig. 4. Comparison of (a) ENDOR of chlorophyll *a* (compound 1) with (b) ENDOR of methyl pyrochlorophyllide *a* (compound 9). The lower scale of each spectrum is labeled such that coupling constants of each peak *A* can be read directly in megahertz. Upper scale of each spectrum is labelled in true units of megahertz frequency shift from the free proton resonance value. In other words, one unit of the upper scale corresponds to two units of the lower scale. Notice that ENDOR spectra are not first derivatives.

significant changes in the ENDOR spectrum. Mirror-image compounds of **9c**(see Table 4) that contain protons in the α, δ and 10 position (the latter only to about 50%) exhibit ENDOR spectra with a single unresolved ENDOR line corresponding to $A \simeq 0.5$ Mz with a shoulder at $A = 1.67$ MHz. Thus, some or all these sites may contribute to the A_1 line in Chl *a* (Compound 1). Similar low-spin density for the β-H is indicated by an exchange experiment with ^{2}H-Chl *a*. Insertion of ^{2}H at β, δ, and 10-H positions of Chl *a* can be accomplished with a reversible Krasnovskii photoreduction of ^{2}H-Chl *a* with ^{1}H$_2$S.[47] The ENDOR spectrum of such a compound is consistent with couplings ≤ 0.5 MHz.

Information about the 7,8-protons can be obtained from compound **12b**; where A_4 is missing, A_2 intensity is diminished relative to A_1, and A_5 is lacking. Since it is likely that A_2, A_3, and A_4 arise from methyl groups, the A_5 resonance may be due to the 7,8-protons. The A_5 resonance is present and apparently unchanged in all other modified chlorophyllides save one, namely, Compound **11**, indicating that A_5 does not involve the vinyl, C-10,

TABLE 4
Cation ENDOR Proton–Electron Hyperfine Coupling Constants (in MHz) of Chlorophylls and Derivatives[a,b]

Structure number[c]	Compound	A_1	A_2	A_3	A_4	A_5	Remarks
1	Chlorophyll a	0.76	2.83	3.72	7.56	11	
9	Methyl pyrochlorophyllide a						
9a	Normal isotopic composition	0.81	3.02	3.81	7.22	10.9	Protic solvent
9b	$5\text{-}C^2H_3$, $10\text{-}C^2H_2$	n.v.	2.83	3.50	—	7–10	
9c	Only: -H, -H, $10\text{-}CH_{2/2}$	0.5/1.67 (sh)	—	—	—	—	
12	Methyl 7,8-*trans*-mesopyrochlorophyllide a						
12a	Normal isotopic composition	0.65	2.77	3.69	7.25	11.1	2-Vinyl missing
12b	$3,5\text{-}C^2H_3$, $7,8\text{-}^2H$	0.62	3.0	—	—	—	$1\text{-}CH_3$, $2,4\text{-}CH_2$, partly exchanged
12c	$3,5\text{-}C^1H_3$, $7,8\text{-}^1H$ only	0.26	2.40	2.92	7.06	10	$1\text{-}CH_3$, $2,4\text{-}CH_2$, partly exchanged
11	Methyl 7,8-*cis*-mesopyrochlorophyllide a	0.57	2.52	3.35	6.45	8/19.8	
10	Methyl 9-deoxomesopyrochlorophyllide a	1.44	2.91	3.54	8.26	11.5	No 9-CO, 2-vinyl
17	10-Hydroxychlorophyll a	n.v.	3.30	—	7.34	n.v.	Protic solvent
14	Chlorin e_6 trimethyl ester	0.68	2.37	2.76	5.88	7.08	Ring V opened
13	Rhodochlorin dimethyl ester	0.44 (sh), 0.98	2.77	3.54	4.69	8 (?)	No γ substituent
15	Isochlorin e_4 dimethyl ester	0.44 (sh), 0.86	3.16	3.91	—	7.69	No 6 substituent
16	Bacteriochlorophyll a	1.4	5.0	—	9.2	14	

[a] Cations were produced by oxidation with I_2 in $C^2H_2Cl_2/C^2H_3O^2H$. See Schemes 1 and 2 for preparation method and structural formulas.

[b] Abbreviations: sh, shoulder; n.v., not visible.

[c] The structure numbers refer to those given in Scheme 2.
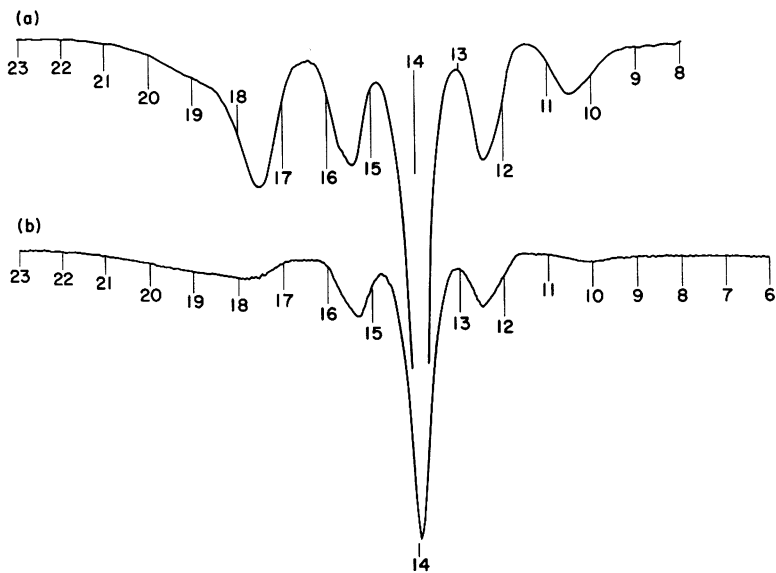
Fig. 5. Comparison of cation of methyl pyrochlorophyllide a oxidized with I_2 (a) of ordinary isotopic composition with 5-C $^2H_3$-methyl pyrochlorophyllide (b) at $\sim 100\,°K$. Note that in (b) the set of ENDOR peaks near 17.5 and 10.5 MHz (i.e., the A_4 resonances) are essentially absent in comparison with (a). The intense center peak near 14 MHz is at approximately the free proton resonance frequency and in this case arises from proton in the solvent (i.e., matrix ENDOR).

or methine protons, and thus an assignment of this peak to the 7,8-protons appears likely.[45] Compound **11** shows a pronounced change in the A_5 resonance. (See Fig. 6a). In compound **11** the 7- and 8-protons are cisoid to each other as opposed to the transoid configuration present in the chlorophylls and normal chlorophyllides. Thus, Compound **11** is a stereoisomer of the meso chlorophyllide **12**. A coupling of $A = 19.9$ MHz is observed in the ENDOR spectrum of Compound **11**, and this large coupling leads to a doublet in the esr spectrum reflecting the $A \approx 20$ MHz. The multiplicity of the esr signal proves that one proton is involved. The ^1H nmr spectrum of Compound **11** indicates pronounced conformational changes in ring IV, while the ^1H nmr resonances of the remaining protons in the molecules are less perturbed.[47] As the pronounced configuration and conformational changes of ring IV are most likely responsible for this new coupling, the assignment to the "extra hydrogens" at C-7 and C-8 was made. This strongly suggests that the similarly large[46] and broadened A_5 resonance in the 7,8-transoid chlorophyllides arises as well from these protons.

The coupling constant of the 2-vinyl group with three α protons can be studied by reduction of the vinyl group (as in Compound **12**) to a 2-ethyl
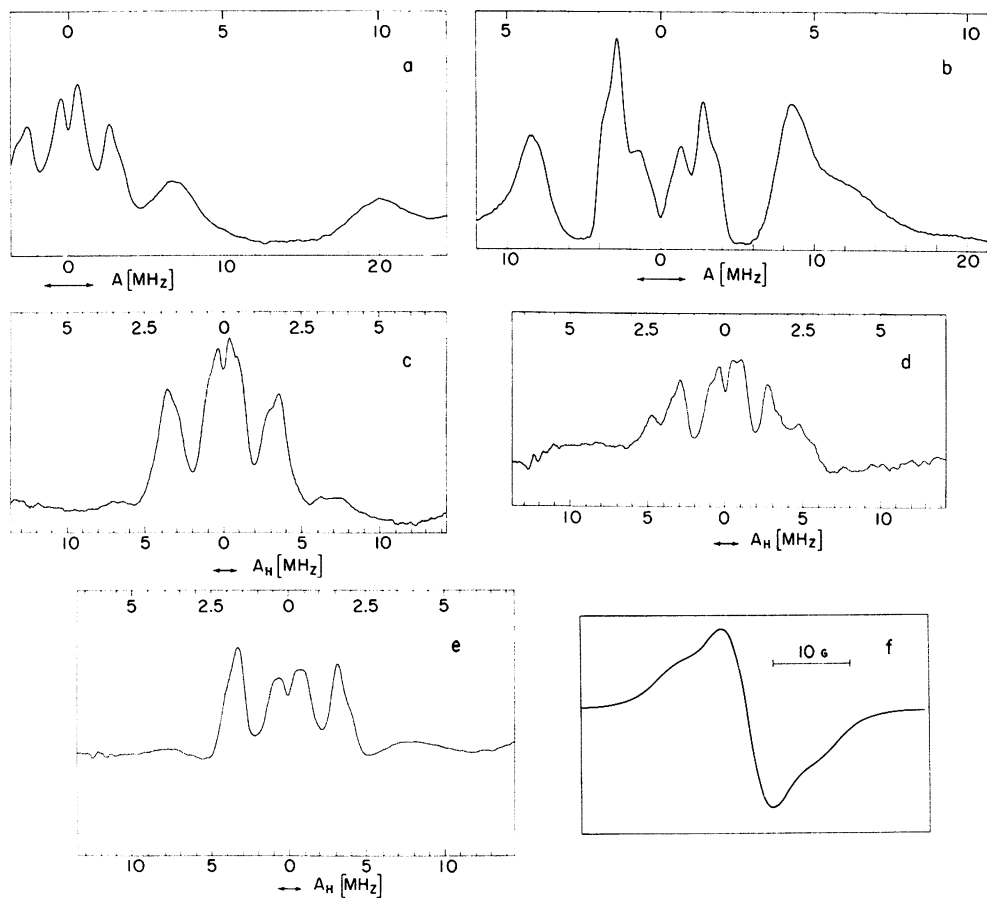
Fig. 6. ENDOR spectra of (a) racemic methyl 7,8-*cis*-mesopyrochlorophyllide *a* (compound 11), (b) racemic methyl 9-deoxomesopyrochlorophyllide *a* (compound 10), (c) chlorin-e_6-trimethyl ester-Mg (compound 14), (d) rhodochlorin-dimethyl ester-Mg (compound 13), (e) Isochlorin e_4 dimethyl ester-Mg (compound 15), (f) esr spectrum of rhodochlorin dimethyl ester-Mg (compound 13). (See the ENDOR spectrum in Fig. 6d.) For convenience the lower scale of each ENDOR spectrum is labeled such that coupling constants of each peak *A* can be read directly in megahertz. The upper scale of each spectrum is labeled in true units of megahertz frequency shift from the free proton resonance value. In other words, one unit of the upper scale corresponds to two units of the lower scale. Although these are typical ENDOR spectra for these compounds and are judged suitable for display purposes, it should be noted that the nonlinear aspects of ENDOR spectroscopy are important when comparing Fig. 6 with Table 4. Table 4 represents the results of many ENDOR spectra and is thus more complete.

group. Consequently, two new beta protons are introduced into the molecule. A_2 now develops a new shoulder, whereas the remainder of the spectrum is for the most part unchanged. Neglecting possible spin redistribution due to reduction of the vinyl group (justified by the negligible changes in other parts of the spectrum) the new shoulder likely results from the new 2-CH_2 group rather than from a change in the coupling constant giving rise to A_2. At the same time a change in A_1 also occurs. The A_1 peak is surely a super-position of several unresolved couplings, and thus A_1 is an approximate mean value only. The pronounced increase (0.38 versus 0.65 MHz) on hydrogenation of the 2-vinyl group in compound 1 to a 2-ethyl group in compound 12 may indicate that the predominant component of this reso-nance has a very small coupling in 1. This indicates a small coupling con-stant for $A \leq 0.38$ MHz for one or more of the vinyl protons. If any of the vinyl protons has a larger coupling constant, it can easily go undetected as resonances from alpha protons are broad and very weak in comparison with those from beta protons, especially rotating methyl or ethyl groups.

The coupling constant of the 10-proton(s) is believed small or else is un-observable. This is concluded because of the similarity of the ENDOR spectra of methylpyrochlorophyllide a, Compound (9), and of Chl a (1). Chloro-phyll a itself has one 10-H, whereas Compound (9) has two 10-protons.

The very different magnitude of the 5-CH_3 hf constant and the 1,3-CH_3 hf constants has been investigated through chemical alteration of ring V of Chl a type compounds. The cation radical of bacteriochlorophyll a (Bchl a) Compound 16, shows a similar methyl group spin density difference. Theory has not predicted these spin density differences in the 1- and the 5-methyl groups, particularly for bacteriochlorophyll. Since bacteriochlorophyll a has two carbonyl groups conjugated to the aromatic π system of the macro-cycle, no vinyl group, and a reduced ring II, the consequent asymmetry in structure likely involves ring V. Ring V is again implicated in the discrepancy by the spectrum of 9-deoxychlorophyllide, Compound 10 (Fig. 6b), which lacks both the 9-carbonyl as well as the 2-vinyl group. Other compounds listed in Table 4 indicate the effect of the vinyl group on the ENDOR spectra to be negligible. The ENDOR spectrum of Compound 10 reveals that A_2 and A_4 resonances (see Table 4) are strongly increased in intensity, but the asymmetry of the methyl resonances also increases.

In contrast, in compounds without the isocyclic five-membered ring (ring V), the two sets of methyl peaks in the ENDOR spectrum gradually move together. [See Compounds 14 (ENDOR spectrum in Fig. 6c), 13 (ENDOR spectrum in Fig. 6d), and 15 (ENDOR spectrum in Fig. 6e).] For isochlorin e_4 (Compound 15) both methyl group signals appear to have merged. Thus, it would appear that the presence of the isocyclic ring has a large effect on the 5-methyl ENDOR resonance. The ENDOR assignments for chlorophyll a type cation radicals is summarized in Table 5. The assignments listed in

TABLE 5
Chlorophyll *a* Spin Densities Derived
From ENDOR Studies on Chlorophyll
***a* Derivatives[a]**

Group[b]	A (G)	nA^{2c} (G^2)	$\lvert\rho_i\rvert^d$
1-CH$_3$	1.0	3.0	0.030
2a-H	0.14	0.02	0.005
2b-H$_{A,B}$	0.14	0.04	0.005
3-CH$_3$	1.31	5–18	0.039
4-CH$_3$	1.0	2.0	0.030
5-CH$_3$	2.67	21.4	0.080
10-H	0.60	0.36	0.018
7-H	3.89	15.11	0.116
8-H	3.89	15.11	0.116
α-H	0.18	0.03	0.007
β-H	0.18	0.03	0.007
δ-H	0.18	0.03	0.007

[a] These results are from Scheer *et al.*[43]

[b] See Fig. 1 for the structural numbering system.

[c] According to Eq. (9) we can calculate ΔH by summing all A_i^2. ^{2}H isotope experiments indicate that the ^{1}H protons contribute ~ 76 G^2 to this sum. The sum of this column is 62.31 G^2 and on this basis these assignments appear reasonable.

[d] Spin density ρ_i is obtained from the respective coupling constants by using Eq. (1) and the following Q values: $Q = 27$ G/spin for alpha protons, $Q = 33.5$ G for beta protons.

Table 5 depend heavily on the ENDOR splittings observed in the many chlorophyll derivatives listed in Table 4.

C. Methyl Group Assignments

The ENDOR investigation and assignment of chlorophyll radicals may also employ a physical as opposed to a chemical approach. The physical approach takes advantage of the special ENDOR properties of methyl groups.[11] Beta methyl protons are known to give prominent, narrow bell-shaped ENDOR resonances.[19,46] The narrow ENDOR line shape is a result of a large ($\sim 90\%$) isotropic component in the beta hyperfine coupling constants. ENDOR experiments have been done primarily on randomly oriented,

frozen-in molecules, and as many as six ENDOR transitions would be observed if a particular methyl group does not rotate rapidly on an esr time scale (rotation of the order of the hyperfine coupling constant). Methyl groups are expected to undergo fast rotations even at 80°K, and thus it is expected that the prominent ENDOR resonances in both Chl a and Bchl a free radicals are from rotating methyl groups. Support of this assignment is provided by low-temperature studies in which near liquid helium temperatures are used to eliminate methyl group rotation. Thus, at 80°K a single set of ENDOR lines is observed because fast methyl rotation makes all three protons equivalent (Fig. 7). At much lower temperatures, a maximum of three sets of lines is expected. In practice a dramatic broadening of the major resonances in Bchl$^+$ and several ENDOR lines is seen at very low temperatures in qualitative agreement with hindered rotation.[11] The resolution depends on many factors, and thus not all lines are expected to be resolved. Under the same circumstances the esr linewidth increases, in good agreement with predictions about hindered rotation. The most pronounced case of hindered rotation occurs in deuterated bacteriochlorophyll in which approximately half the methyl protons are replaced by deuterons.[11] The heavier mass of ^2H is expected to have a large effect on hindered rotation. An unfortunate consequence of hindered rotation is a large decrease in the intensity of the ENDOR transitions. In fact, it is the rapid rotation of the methyl groups that helps provide such a favorable ENDOR mechanism for these beta protons. Thus, "fixed" beta protons, for example the 7- and 8-H, although very isotropic in hyperfine nature, also are expected to be weak in intensity since they are limited to vibrational motions only.
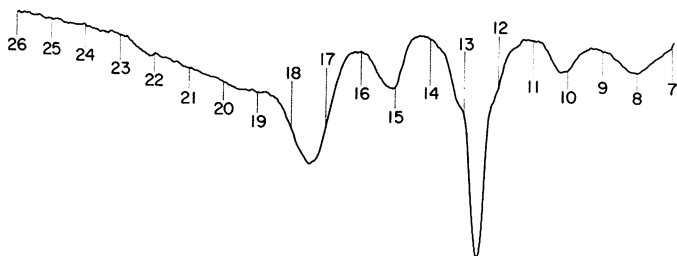
Fig. 7. Typical ENDOR spectrum of monomeric bacteriochlorophyll a cation produced by oxidation with I_2 in 3:1 volume/volume $CH_2Cl_2 - CH_3OH$. The following identifications are made: A_1 and the shoulders near 12 and 13 MHz; A_2 and the peaks near 15.2 and 10.3 MHz; A_3 is considered not applicable; A_4 and peaks near 17.5 and 8 MHz; A_5 and the wing from 19 to 22 MHz. Since the solvent is not deuterated, a large center peak, the matrix ENDOR peak, falls near the free proton frequency of 12.6 MHz. The free proton frequency is experimentally variable, depending on what value of microwave frequency is used in the ENDOR experiment. Had a higher microwave frequency been employed, the free proton frequency would have been higher (typically 13.7–14 MHz) and the low frequency half of the A_5 peaks would have been observable.

Thus, in Chl a the major endor resonances (A_2 and A_4) arise from methyl groups as deduced from chemical evidence. In Bchl† physical evidence exists that also suggests that the two sets of intense, narrow ENDOR lines arise from methyl groups. In Bchl† only the 1- and 5-CH$_3$ protons can reasonably be expected to qualify as the source of these resonances. On the basis of deuteration effects on the 5-CH$_3$ in pyrochlorophyllide a, we also expect the 5-CH$_3$ of Bchl† to have the larger coupling constant.

D. Biosynthetic Isotopic Labeling

Fortunately more can be done to confirm the methyl group assignments in Bchl systems.[10-12] Selective deuteration of the methyl groups is possible by biosynthetic techniques developed by Katz et al.[44,45] To accomplish this, deuterium is selectively introduced into Bchl a in vivo by growing Rhodospiril-lum rubrum in ^{2}H$_2$O plus succinic acid-^{1}H$_4$, which serves as the required carbon source. ^{1}H nmr has shown that organisms grown in this nutrient medium produces Bchl containing ^{2}H at all of the methine positions and at positions 3, 4, 7, and 8. In contrast, R. rubrum grown in ^{1}H$_2$O on succinic acid-d_4 contains Bchl with ^{1}H at positions 3, 4, 7, and 8 and at the methine proton positions. In both cases, the 1a- and 5a-CH$_3$ groups contain both ^{1}H and ^{2}H. With the organisms grown in ^{2}H$_2$O, the 1a- and 5a-methyl groups dominate the ENDOR spectrum and thus the assignments are easily made. In vitro Bchl a biosynthetically deuterated except in the 1a- and 5a-methyl groups still exhibits the same peaks near 19 and 16.7 MHz, and thus those peaks must arise from the 5a- and 1a-CH$_3$ groups (Fig. 8). In the mirror image experiment, the 3, 4, 7 and 8 positions contain $\sim$100% ^{1}H and the 5a- and 1a- Chl$_3$ are roughly 50% in ^{1}H. Thus, this selectively deuterated species gives rise to an ENDOR spectrum in which the peaks near 19 and 16.7 MHz are weak in intensity relative to the peak near 22 MHz (A_5). Both experiments indicate that the prominent resonances arise from the methyl groups and the wing A_5 arises from either the 3-, 4-, 7-, and 8-protons or the methine protons. It is very unlikely that the methine protons would be involved in the A_3 resonances since α protons are expected to be too broad and weak to be detected because of the large anisotropy in the hyperfine interactions. It should be noted additionally that theory predicts high-spin density at the 3-, 4-, 7-, and 8-hydrogens and very low-spin density at the methine hydrogens.

In order to confirm the expected low-spin density at the methine positions and the high spin density at the fixed β protons, chemical exchange of ^{1}H for ^{2}H may again be used. ^{2}H-Bchl a dissolved in methanol was exchanged in the presence of a small amount of CF$_3$COOH, which results in 100% exchange of the C-10 proton, and $\sim$90% exchange of one methine proton,
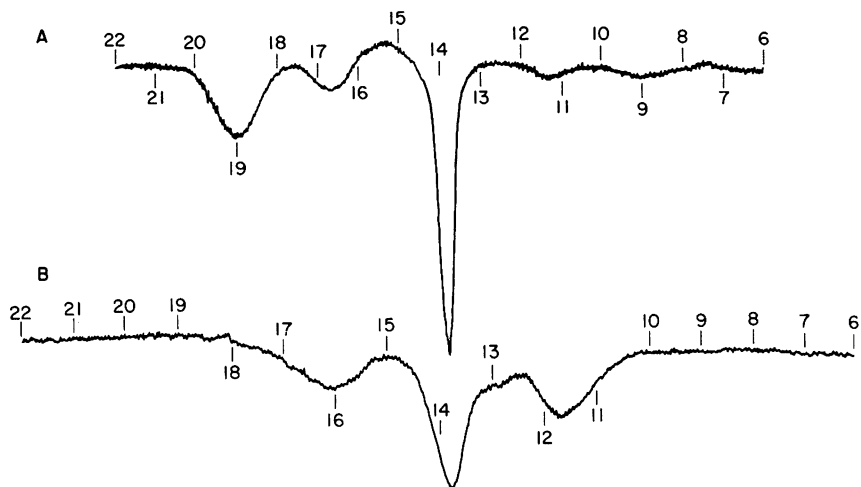
Fig. 8. Comparison of endor of bacteriochlorophyll free radicals containing ENDOR active protons only at the 1-CH_3 and 5-CH_3 positions for both *in vivo* and *in vitro* systems at $\sim 100°$ K. (A) *In vitro*: A_4 near 19 MHz and 9 MHz; A_1 near 16.7 and 11.3 MHz. (B) *In vivo*: A_4 near 16.0 and 11.8 MHz; A_1 near 14.7 and 12.9 MHz.
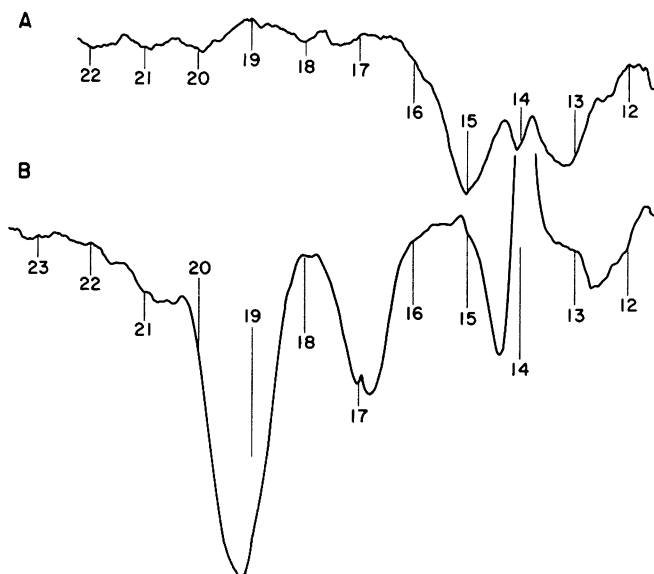
Fig. 9. Endor spectra of ^{1}H-exchanged ^{2}H-Bchl‡ oxidized by I_2 in $C^2H_3O^2H-C^2H_2Cl_2$, 1:3 (volume/volume). (A) Normal gain; (B) Ten times normal gain.

TABLE 6
Comparison of *in Vitro* and *in Vivo* ENDOR Data for Bacterial Systems

| Protons[a] | Hyperfine coupling constants (MHz) | | Aggregation number[b] | Ref. |
	BChl $a^{\ddagger}$	*In vivo*		
$(\alpha, \beta, \delta, 10)$	c	c	c	11
	1.4	0.8	1.7	12
1a	5.0 ± 0.1	2.0 ± 0.1	2.5	11
	5.32	2.2	2.4	12
5a	9.2 ± 0.2	4.2 ± 0.2	2.2	11
	9.8	4.7	2.1	12
$(7, 8, 3, 4)$	16	8	2.0	11
	14	7	2.0	12
Average			$2.1 \pm .3$	

[a] Proton numbering from Fig. 1B. Parentheses indicate the coupling constant arises from some or all of the indicated groups.

[b] Aggregation number = ratio of coupling constants *in vitro* to coupling constants *in vivo*. See Eq. (10).

[c] Not available.

$\sim 65\%$ exchange of another methine proton, and $\sim 20\%$ exchange of the methyl groups at positions 1, 2b, and 5 as established by ^{1}H nmr. The ENDOR results of this experiment are shown in Fig. 9. Spectrum A in Fig. 9 is recorded at normal gain ($\times 1$) and reveals resonance near the free proton frequency (14 MHz). Spectrum B in Fig. 9 is recorded at high gain ($\times 10$) and at a magnetic field that optimizes response to the methyl group resonances near 19 and 17 MHz. These prominent methyl peaks in Fig. 9B are present in Fig. 9A also but are obscured by noise. Thus, we know that the resonance observed in spectrum A results from the exchanged methine protons and/or the C-10 protons in accordance with our expectations about the role of alpha versus beta protons in the genesis of A_5.

We are thus in a position to summarize the findings on *in vitro* ENDOR assignments and *in vitro* spin density in Table 6.

VI. *IN VIVO* ENDOR OF THE PHOTOSYNTHETIC APPARATUS

The primary purpose of investigating the chlorophylls by ENDOR spectroscopy is to establish the validity of the special pair model for photoreaction center chlorophyll. In the simplest context verification of the special pair

model requires comparison of a set of coupling constants *in vitro* and *in vivo*. If the special pair model is correct, then for each hyperfine coupling observed in an *in vitro*, monomeric chlorophyll cation free radical a corresponding coupling constant of one-half the monomer value will be observed *in vivo* [in accordance with Eq. (10), where $N = 2$]. Proof also requires molecular assignment of the *in vivo* ENDOR transitions. Both of these goals can be attained in a straightforward fashion in purple photosynthetic bacteria *Rhodospirillum rubrum* and *Rhodopseudomonas spheroides*. The molecular assignments of the ENDOR coupling constants are possible because of the selective deuteration of Bchl *a in vivo* by the biosynthetic method discussed above in Section V,D. The ENDOR spectra of Bchl$^+$ monomer and the corresponding *in vivo* signal can be readily interpreted, whereas the ENDOR spectra of green or blue-green algae and of Chl a^+ monomer are much more complicated (presumably owing to hindered motion of methyl groups *in vivo*) and therefore are more difficult to compare. Additional complications result in green plants because a biosynthetic method to deuterate properly and selectively Chl *a in vivo* does not exist at present.

A.   ENDOR Evidence for the Special Pair in Photosynthetic Bacteria

The ENDOR spectra of *in vivo* and *in vitro* bacterial systems are compared in Fig. 10. The data in Table 6 indicate that the special pair model can indeed be used to interpret the *in vivo* ENDOR. The special pair concept requires all aggregation numbers *in vivo* to be near the value of two. Table 6 shows the remarkable agreement in the experimentally determined aggregation numbers *in vivo* whose average value is very close to 2.

As previously mentioned, such a comparison of *in vitro* and *in vivo* ENDOR hyperfine data from which an aggregation number of two is deduced would be much more satisfying if the *in vivo* and *in vitro* hyperfine splittings could be assigned independently. Since we have already discussed the *in vitro* assignments, all that remains for discussion are the results of biosynthetic deuteration of Bchl *a in vivo*. First, the ENDOR of photooxidized bacteria grown in ^2H_2O with succinic acid-$^1H_4$ is observed. As previously discussed, only the 1- and 5-methyl protons can give rise to significant ENDOR resonances in these systems. (The *in vivo* ENDOR is illustrated in Figs. 8B and 11.) Note the absence of A_5 and the prominence of A_2 and A_4 in these spectra. We take this as chemical evidence of the assignment of the 1- and 5-methyl groups to these prominent resonances in agreement with the hindered rotation studies. In the isotopic mirror image experiment, bacteria are grown in ^1H_2O on succinic acid-d_4, so that all positions contain ^1H, but the 1- and 5-CH$_3$ groups are roughly half-deuterated in comparison with the
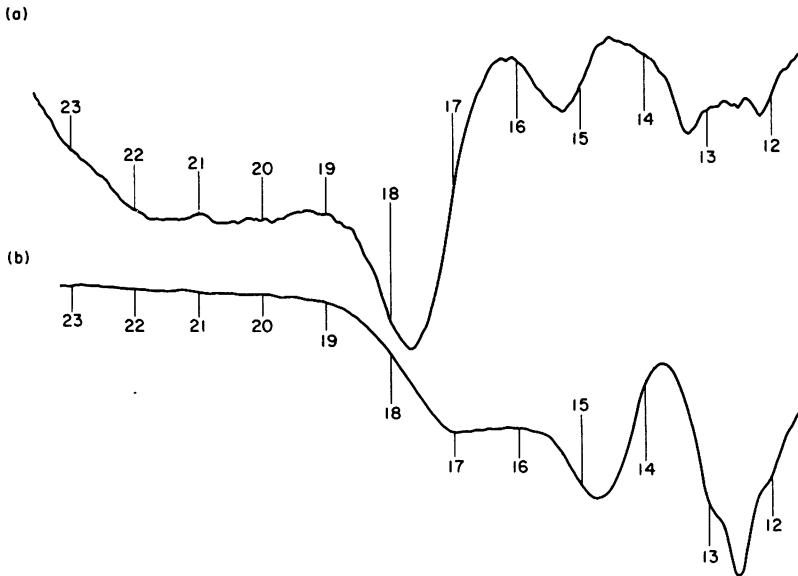
Fig. 10. Comparison of Bchl$^+$ (a) with *in vivo R. rubrum*; (b) ENDOR. *In vitro* signal generated by I_2 in $C^2H_3O^2H-C^2H_2Cl_2$, 1:3 (volume/volume). *In vivo* signal generated by $K_3Fe(CN)_6$. Temperature $\cong$ 15 K.
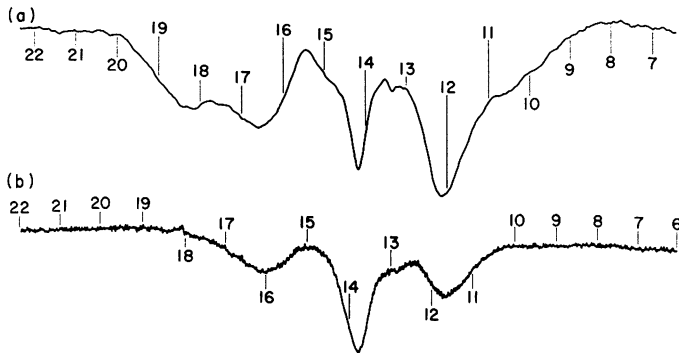
Fig. 11. Mirror image experiment of Fig. 8b: (a) ^1H *R. rubrum* grown on ^2H succinate, whole cells oxidized with $K_3Fe(CN)_6$; (b) ^2H *R. rubrum* grown on ^1H succinate, whole cells oxidized with $K_3Fe(CN)_6$. Notice that the A_5 peaks (18.3 and 10.5 MHz) are relatively large since the A_2 and A_4 peaks have diminished ^1H concentration.

3, 4, 7, and 8 and methine positions, which contain only ^1H. The ENDOR spectrum of this isotopic mirror image bacteria is shown in Fig. 11. These data show that the peaks assigned to the methyl groups are considerably down in intensity relative to the remainder of the spectrum as required from the partial deuteration of the 1- and 5-CH$_3$ groups.

The evidence that two chlorophyll molecules share the unpaired electron almost equally in photooxidized reaction centers at low temperatures appears overwhelming. As the esr linewidth remains near 9 G at room temperature, it seems most probable that two molecules of Bchl a truly function $in\ vivo$ as the unit of oxidized Bchl a. The overall evidence supports the concept that a special pair of bacteriochlorophyll a molecules constitutes the primary donor unit of bacterial photosynthesis in the systems so far studied by esr and ENDOR. We recommend the use of the term "special pair," symbol Chl_{sp} or $Bchl_{sp}$ instead of "dimer." Dimer refers to $(Chl)_2$, a species in which the chlorophylls are linked by a coordination interaction between the keto $C{=}O$ function of one chlorophyll molecule and the Mg of another: keto $C{=}O \cdots Mg$. This is fundamentally a different structure from that of Chl_{sp}.

B.   ENDOR of Green Oxygen-Evolving Plants

We now return to the question of the ENDOR observed in oxidized algae (a Vernon P-700[48] preparation). Since we cannot make assignments by biosynthetic means, we must depend on comparisons of the $in\ vivo$ ENDOR spectra with $in\ vitro$ spectra by the special pair concept (Fig. 12). Applying Eq. (10), we can successfully interpret the $in\ vivo$ ENDOR data in terms of an aggregation number of two and the monomeric $in\ vitro$ Chl a cation
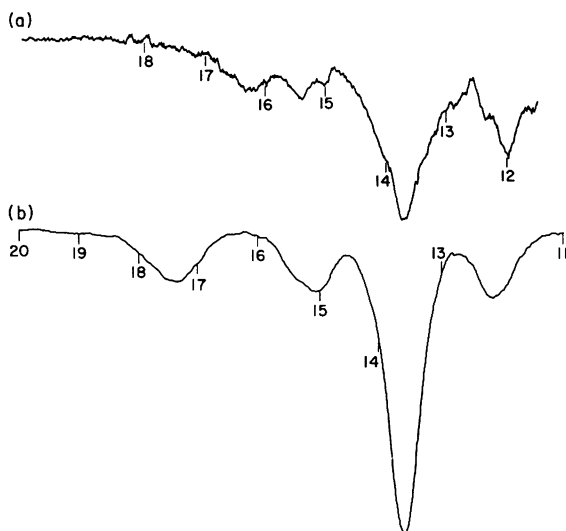
Fig. 12. Comparison of Chl a^+ (b) with $in\ vivo$ S. $lividus$ (a) oxidized by $K_3Fe(CN)_6$ at 108°K. $In\ vitro$ signal generated by I_2 in $CH_3OH-CD_2H_2$ (4:1).

TABLE 7

Comparison of *in Vitro* and *in Vivo* ENDOR Data for Plant Systems[a]

| Protons[b] | Hyperfine coupling constants (MHz) | | Aggregation number[c] |
	Chl a^{+}	*In vivo*	N
(1a, 3a, 4a)	3.19	1.7	1.9
	3.72		2.2
5a	7.45	3.73	2.0
(7, 8)	11.8	5.4	2.2
Average			2.1

[a] This data is from Norris *et al.*[4] See also Feher *et al.*[11]

[b] Proton numbering from Fig. 1a. Parentheses indicate the coupling constant is assumed to arise from some or all of the indicated groups.

[c] N is determined by Eq. (10).

hyperfine coupling constants (as summarized in Table 7). The *in vivo* data for green plants exhibit more structure in the ENDOR spectra than do the *in vitro* data and the intensities as well as the magnitude of the coupling constants are such that it is likely that hindered rotation occurs at temperature above 80°K (Fig. 12), although Chl a^{+} *in vitro* appears to exhibit no hindered rotation of the methyl groups at this temperature. The increase in esr linewidth upon freezing algae[12] also suggests hindered rotation *in vivo*. That similar methyl groups behave differently with respect to hindered rotation in different environments is known to be the case from experiment. Thus, the general features of the *in vivo* green plant ENDOR spectra appear at this time to be best interpretable in terms of two chlorophyll molecules approximately sharing an unpaired electron, that is, special pairs.

Various structures have been advanced for the chlorophyll special pair in which water serves as the orienting agent.[2,4,8,49] More recently a model for Chl_{sp} has been advanced in which nucleophilic OH, NH_2, or SH groups in protein side chains are used in the organization of the special pair, thus providing for protein participation in the formation of the photoreaction center.[50]

VII. CONCLUSION

In the photosynthetic organisms that have been extensively studied up to the present, doublet free radicals are produced in the primary act of photosynthesis that arise from a special pair of chlorophyll molecules. ENDOR spectroscopy has provided powerful evidence in support of this view, particularly in certain photosynthetic bacteria.

REFERENCES

1. G. Feher, *Phys. Rev.* **103**, 834–835 (1956).
2. J. J. Katz, K. Ballschmiter, M. Garcia-Morin, H. H. Strain, and R. A. Uphaus, *Proc. Nat. Acad. Sci. U.S.* **60**, 100–107 (1968).
3. M. Garcia-Morin, R. A. Uphaus, J. R. Norris, and J. J. Katz, *J. Phys. Chem.* **73**, 1066 –1070 (1969).
4. J. R. Norris, R. A. Uphaus, H. L. Crespi, and J. J. Katz, *Proc. Nat. Acad. Sci. U.S.* **68**, 625–629 (1971).
5. J. D. McElroy, G. Feher, and D. C. Mauzerall, *Biochim. Biophys. Acta* **267**, 363–374 (1972).
6. J. R. Norris, R. A. Uphaus, and J. J. Katz, *Biochim. Biophys. Acta* **275**, 161–168 (1972).
7. G. Feher, A. J. Hoff, R. A. Isaacson, and J. D. McElroy, *Biophys. Soc. Abstr.* **13**, 61a (1973).
8. J. J. Katz and J. R. Norris, *in* "Current Topics in Bioenergetics" (D. R. Sanadi and L. Packer, eds.), pp. 41–75. Academic Press, New York, 1973.
9. J. R. Norris, M. E. Druyan, and J. J. Katz, *J. Am. Chem. Soc.* **95**, 1682–1683 (1973).
10. J. R. Norris, H. Scheer, and J. J. Katz, *Ann. N. Y. Acad. Sci.* **244**, 261–280 (1975).
11. G. Feher, A. J. Hoff, R. A. Isaacson, and L. C. Ackerson, *Ann. N.Y. Acad. Sci.* **244**, 239–259 (1975).
12. J. R. Norris, H. Scheer, M. E. Druyan, and J. J. Katz, *Proc. Nat. Acad. Sci. U.S.* **71**, 4897– 4900 (1974).
13. J. E. Wertz and J. R. Bolton, *in* "Electron Spin Resonance — Elementary Theory and Practical Applications," p. 497. McGraw-Hill, New York, 1972.
14. H. M. Swartz, J. R. Bolton, and D. C. Borg, (eds.), "Biological Applications of Electron Spin Resonances." Wiley (Interscience), New York, 1972.
15. H. M. McConnell, *J. Chem. Phys.* **24**, 764–766 (1956).
16. R. Bersohn, *J. Chem. Phys.* **24**, 1066–1070 (1956).
17. S. I. Weissman, *J. Chem. Phys.* **25**, 890–891 (1956).
18. H. M. McConnell and D. B. Chestnut, J. Chem. Phys. **28**, 107–117 (1958).
19. J. S. Hyde, "Magnetic Resonance in Biological Systems" (*Proc. Int. Conf., 2nd, Wenner-Gren Center, Stockholm, Sweden, June 1966*). Pergamon, Oxford, 1967.
20. B. Commoner, J. J. Heise, and J. Townsend, *Proc. Nat. Acad. Sci. U.S.* **42**, 710–718 (1956).
21. P. Sogo, M. Jost, and M. Calvin, *Radiat. Res. Suppl. I* 511–518 (1959).
22. J. H. Fuhrhop and D. C. Mauzerall, *J. Am. Chem. Soc.* **91**, 4174–4181 (1969).
23. J. D. McElroy, G. Feher, and D. C. Mauzerall, *Biochim. Biophys. Acta* **172**, 180 (1969).
24. J. Fajer, D. C. Borg, A. Forman, D. Dolphin, and R. H. Felton, *J. Am. Chem. Soc.* **92**, 3451–3459 (1970).
25. D. C. Borg, J. Fajer, R. H. Felton, and D. Dolphin, *Proc. Nat. Acad. Sci. U.S.* **67**, 813–820 (1970).
26. J. Fajer, D. C. Borg, A. Forman, R. H. Felton, D. Dolphin, and L. Vegh, *Proc. Nat. Acad. Sci. U.S.* **71**, 994–998 (1974).
27. J. R. Bolton, R. K. Clayton, and D. W. Reed, *Photochem. Photobiol.* **9**, 209–218 (1969).
28. D. H. Kohl, J. Townsend, B. Commoner, H. L. Crespi, R. C. Dougherty, and J. J. Katz, *Nature (London)* **206**, 1105 (1965).
29. L. N. M. Duysens, *in* Transfer of Excitation Energy in Photosynthesis. Ph.D. thesis, State Univ., Utrecht, The Netherlands, 1952.
30. B. Kok, *Plant Physiol.* **34**, 184–192 (1959).
31. J. D. McElroy, D. C. Mauzerall, and G. Feher, *Biochim. Biophys. Acta* **333**, 261–277 (1974).
32. J. T. Warden and J. R. Bolton, *J. Am. Chem. Soc.* **95**, 6435 (1973).
33. J. T. Warden and J. R. Bolton, *Accounts Chem. Res.* **7**, 189–195 (1974).

34. P. A. Loach and D. L. Sekura, *Photochem. Photobiol.* **6**, 381–393 (1967).
35. M. G. Rockley, M. W. Windsor, R. J. Cogdell, and W. W. Parson, *Proc. Nat. Acad. Sci. U.S.* **72**, 2251–2255 (1975).
36. K. J. Kaufmann, P. L. Dutton, T. L. Netzel, J. S. Leigh, and P. M. Rentzepis, *Science* **188**, 1301–1304 (1975).
37. P. L. Dutton, K. J. Kaufmann, B. Chance, and P. M. Rentzepis, *FEBS Lett.* **60**, 275–280 (1975).
38. W. W. Parson and R. J. Cogdell, *Biochim. Biophys. Acta* **416**, 105–149 (1975).
39. T. L. Netzel, J. S. Leigh, and P. M. Rentzepis, *Science* **182**, 238–241 (1973).
40. K. J. Kaufmann and P. M. Rentzepis, *Accounts Chem. Res.* **8**, 407–412 (1975).
41. J. Fajer, D. C. Brune, M. S. Davis, A. Forman, and L. D. Spaulding, *Proc. Nat. Acad. Sci. U.S.* **72**, 4956–4960 (1976).
42. J. J. Katz, *in* "Inorganic Biochemistry" (G. Eichhorn, ed.), p. 1022. Elsevier, Amsterdam, 1973.
43. H. Scheer, J. R. Norris, and J. J. Katz, *J. Am. Chem. Soc.* **99**, 1372–1381 (1977).
44. J. J. Katz, R. C. Dougherty, H. L. Crespi, and H. H. Strain, *J. Am. Chem. Soc.* **88**, 2856 (1966).
45. R. C. Dougherty, H. L. Crespi, H. H. Strain, and J. J. Katz, *J. Am. Chem. Soc.* **88**, 2854–2855 (1966).
46. J. S. Hyde, G. H. Rist, and L. E. Goran Ericksson, *J. Phys. Chem.* **72**, 4269–4276 (1968).
47. H. Scheer and J. J. Katz, *Proc. Nat. Acad. Sci. U.S.* **71**, 1626–1629 (1974).
48. L. P. Vernon, H. Y. Yamamoto, and T. Ogawa, *Proc. Nat. Acad. Sci. U.S.* **63**, 911–917 (1969).
49. F. K. Fong, *Proc. Nat. Acad. Sci. U.S.* **71**, 3692–3695 (1974).
50. L. L. Shipman, T. M. Cotton, J. R. Norris, and J. J. Katz, *Proc. Nat. Acad. Sci. U.S.* **73**, 1791–1794 (1976).